RESEARCH PAPER

Synthesis of absorbent for the removal of heavy metals from waste water

A. Anbu, S. B. Jaivant, M. Rukkesh, D. Deepthavarshan

Department of Chemical Engineering, V.S.B Engineering College Karur, Tamilnadu -639 111.
anbuchemical4@gmail.com, jaivantsb@gmail.com, rukkeshrukkesh179@gmail.com, deepthavarshan@gmail.com

Received: 16th Dec, 2025; Revised: 8th Feb 2026; Accepted: 12th Feb, 2026; Available Online: 28th Feb, 2026

ABSTRACT
The contamination of water resources by heavy metals, particularly hexavalent chromium, has become a significant environmental and public health concern due to its high toxicity, carcinogenic nature, and persistence in aquatic systems. In the present study, a low-cost and environmentally sustainable adsorbent was synthesized from Wrightia tinctoria leaves through chemical activation using phosphoric acid. The prepared biomass was subjected to controlled Carbonization at 400°C to develop a porous structure with enhanced surface area and active functional groups. The resulting activated Carbon was evaluated for its adsorption efficiency in removing chromium^{+} ions from aqueous solutions using potassium dichromate as a model contaminant. Batch adsorption experiments were carried out by preparing a 100 mL chromium solution containing 0.10 g of potassium dichromate, followed by the addition of 0.10 g of activated adsorbent. The mixture was agitated using a magnetic stirrer for 60 minutes and allowed to settle before filtration. A significant reduction in the characteristic orange colour of the solution was observed, indicating effective removal of chromium ions. The adsorption efficiency was found to be in the range of approximately 85–92%, depending on experimental conditions. The enhanced adsorption performance is attributed to the presence of functional groups such as hydroxyl (–OH) and carboxyl (–COOH), along with increased porosity developed during chemical activation. The results demonstrate that Wrightia tinctoria-based activated Carbon is an effective, low-cost, and eco-friendly adsorbent for the removal of toxic Cr^{6+} ions from wastewater.

Keywords: Biochar, Adsorption, Heavy metal removal, Hexavalent chromium (Cr^{6+}), Wrightia tinctoria, Activated carbon, Wastewater treatment, Phosphoric acid activation

How to cite this article: Anbu A, Jaivant SB, Rukkesh M, Deepthavarshan D. Synthesis of absorbent for the removal of heavy metals from waste water. Int J Drug Deliv Technol. 2026;16(39s): 438-447. DOI: 10.25258/ijddt.16.39s.60.
Source of support: Nil.
Conflict of interest: None

1.INTRODUCTION

Water pollution caused by heavy metals has emerged as one of the most critical environmental challenges in recent years, primarily due to rapid industrialization and urban expansion. Heavy metals such as lead (Pb), cadmium (Cd), mercury (Hg), and chromium (Cr) are non-biodegradable and tend to accumulate in living organisms, leading to severe health risks through bioaccumulation and biomagnification.

Among these, chromium exists mainly in two oxidation states: trivalent chromium (Cr^{3+}) and hexavalent chromium (Cr^{6+}). While Cr^{3+} is relatively less toxic and even considered an essential micronutrient in trace amounts, Cr^{6+} is highly toxic, carcinogenic, and poses serious environmental hazards due to its high solubility and mobility in water. Industrial activities such as electroplating, leather tanning, textile dyeing, and metal finishing are major sources of Cr^{6+} contamination in wastewater. Conventional methods for heavy metal removal, including chemical precipitation, ion exchange, and membrane filtration, often suffer from limitations such as high operational cost, sludge generation, and reduced efficiency at low metal concentrations. In this context, adsorption has gained considerable attention as an effective and economical alternative due to its simplicity, high efficiency, and adaptability.

Activated Carbon is widely used as an adsorbent; however, its commercial production is expensive. This has led to increasing interest in the development of

**Author for Correspondence: A. Anbu*

low-cost adsorbents from natural biomass materials. Lignocellulosic biomass, such as plant leaves, contains functional groups like hydroxyl, carboxyl, and phenolic groups, which can effectively bind heavy metal ions. In the present study, leaves of Wrightia tinctoria, a locally available plant species, were utilized as a precursor for the synthesis of activated Carbon. Chemical activation using phosphoric acid was employed to enhance the surface area and pore structure of the biomass. The prepared adsorbent was then evaluated for its ability to remove Cr^{6+} ions from aqueous solutions using potassium dichromate as a model pollutant.

This study aims to develop a sustainable and cost-effective adsorbent and to evaluate its performance under controlled experimental conditions, thereby contributing to the advancement of efficient wastewater treatment technologies.

2.Materials and Methods

2.1 Preparation of Raw Biomass Material

The raw biomass used for the preparation of the adsorbent was derived from Wrightia tinctoria leaves collected from Mustakinathupatti, Karur District, Tamil Nadu, India. The selection of this biomass was based on its lignocellulosic composition, which is rich in cellulose, hemicellulose, and lignin, providing abundant functional groups suitable for adsorption processes. The collected leaves were initially subjected to thorough washing using tap water for 3–4 cycles to remove loosely bound impurities such as dust, soil particles, and organic debris. This was followed by successive rinsing with distilled water (2–3 cycles) to eliminate soluble inorganic contaminants and residual ions that could interfere with adsorption efficiency.

After washing, the leaves were air-dried under sunlight for approximately 30–60 minutes to remove surface moisture. This preliminary drying step reduces the energy required during oven drying. The partially dried leaves were then cut into small, uniform pieces (1–2 cm) to ensure homogeneous heat distribution during subsequent drying.

The prepared samples were oven-dried at a controlled temperature of 80–100°C for 2–3 hours until a constant weight was achieved, indicating effective removal of moisture. The final moisture content was reduced to below approximately 10%, which is essential to prevent microbial degradation and to enhance the efficiency of the activation process.

The dried biomass was pulverized using a ball mill to obtain fine powder, thereby increasing the surface area available for adsorption. The powder was then sieved to achieve a uniform particle size distribution in the range of 100–200 µm. This uniformity ensures better packing, enhanced surface exposure, and reproducibility in adsorption experiments.

Finally, the processed biomass was stored in airtight containers to prevent moisture absorption and contamination prior to chemical activation.

Wrightia tinctoria plant

Dried leaves

Wrightia tinctoria leaves

Grinded fine powder

Figure 2.1 Raw material

2.2 Preparation of Activated Adsorbent

The adsorbent was synthesized through chemical activation of the prepared biomass using phosphoric acid (H_3PO_4), a widely used activating agent known for its ability to promote pore formation and enhance surface functionality. A predetermined amount of 100 g of powdered biomass was mixed with 100 mL of phosphoric acid, maintaining an impregnation ratio of 1:1 (w/v). The mixture was thoroughly stirred to obtain a homogeneous paste, ensuring uniform distribution of the activating agent throughout the biomass matrix. The beaker containing the mixture was sealed with aluminium foil to prevent contamination and evaporation losses. The impregnation process was allowed to proceed for 24 hours at room temperature. During this period, phosphoric acid penetrates the internal structure of the biomass, facilitating dehydration reactions and breakdown of lignocellulosic components, which is critical for pore development during Carbonization. For thermal treatment, a clay crucible was prepared by coating its outer surface with three successive layers of clay. This coating enhances thermal insulation, minimizes heat loss, and prevents structural damage at high temperatures. Each layer was carefully dried, and cracks were sealed to ensure mechanical stability. The coated crucible was then air-dried for 2–3 days. After impregnation, the treated biomass was transferred into the prepared clay container. The container was sealed with a clay lid, and the joints were tightly packed with clay to create an oxygen-limited environment. This condition is essential to prevent combustion and to ensure proper Carbonization.

The sealed container was placed in a muffle furnace and heated at 400°C for 2 hours. During this process, thermal decomposition of organic matter occurs, resulting in the formation of a Carbon-rich, porous structure. The presence of phosphoric acid promotes cross-linking reactions and inhibits tar formation, thereby increasing the yield and porosity of the adsorbent. After completion of the heating process, the furnace was turned off, and the sample was allowed to cool gradually inside the furnace for 24 hours. This slow cooling prevents thermal shock and preserves the structural integrity of the adsorbent.

The cooled material was then removed and allowed to equilibrate at room temperature for 30–60 minutes before opening the container.

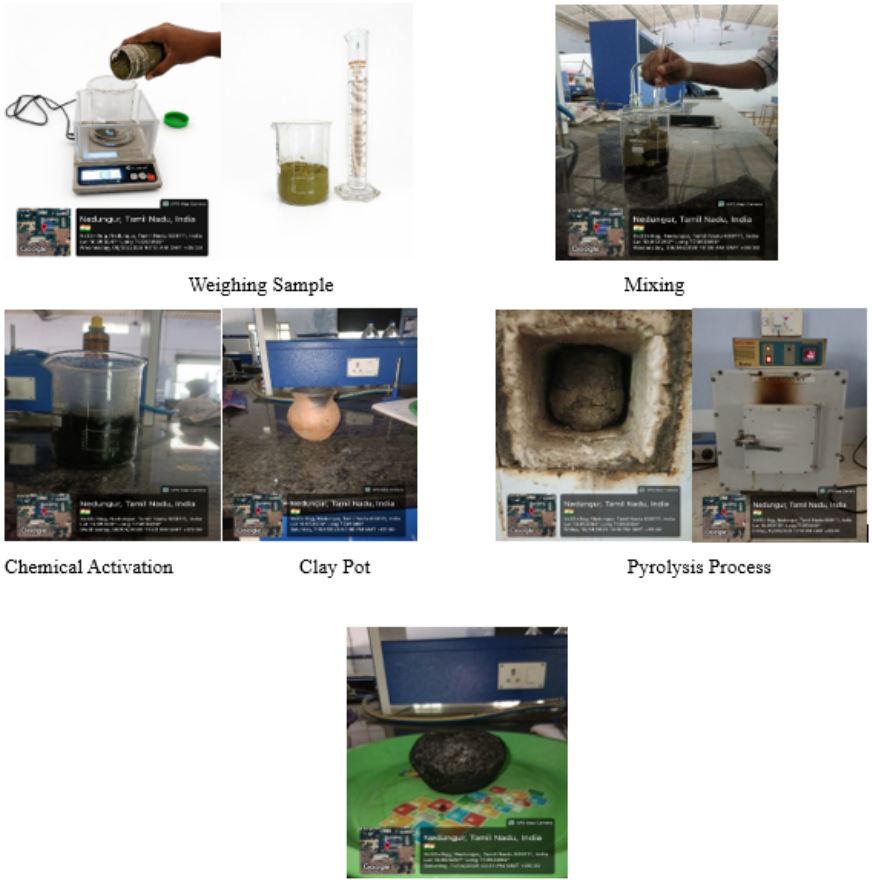

Figure 2.2 Preparation of Activated Carbon

2.3 Washing and Neutralization Process

The activated Carbon obtained after Carbonization contained residual phosphoric acid and soluble impurities. To remove these, the material was repeatedly washed with distilled water. The washing process was continued for approximately 35–40 cycles until the pH of the filtrate increased from an initial value of around pH 1 to near-neutral pH 6.5. Continuous monitoring of pH ensured complete removal of excess acid. This neutralization step is critical, as residual acidity can interfere with adsorption studies and affect the interaction between adsorbent and adsorbate. After achieving neutral pH, the adsorbent was dried and stored in airtight containers for further experimental use.

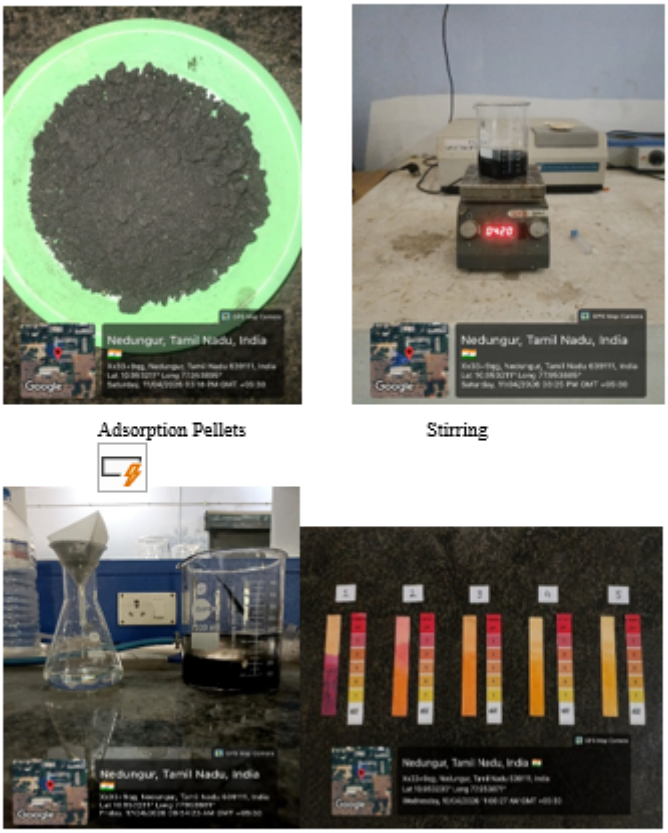

Adsorption Pellets Stirring

Settling and Filtration pH Neutralization

Figure 2.3 Washing and Neutralized process

3. Results and Discussions

3.1 Characterization

3.1.1 FTIR Spectroscopic Analysis

FTIR spectroscopy was performed on CARBON using a Bruker OPUS 7.5.18 instrument over the wavenumber range of 500–4000 cm^{-1}. The transmittance spectrum revealed multiple characteristic absorption bands corresponding to diverse functional groups present on the adsorbent surface. Table 1 summarizes the identified bands, their assignments, and their significance to the adsorption mechanism.

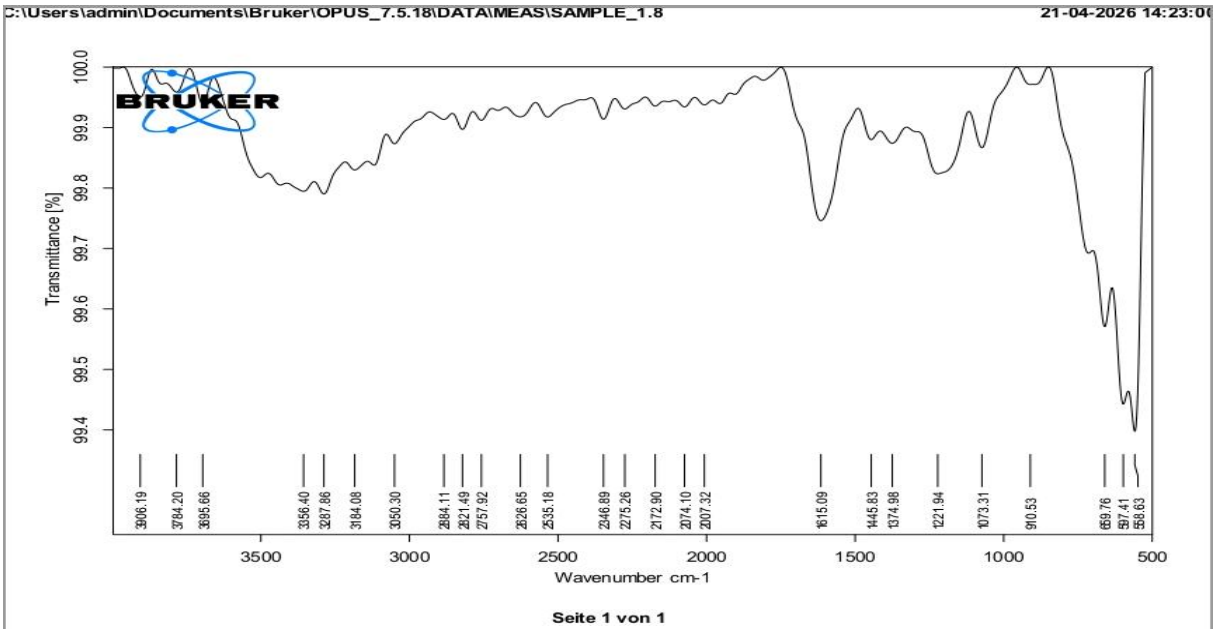

Figure 3.1.1 FTIR Spectroscopic Analysis

3.1.2 FTIR Analysis for CARBON

The broad O–H stretching absorptions observed in the region 3906–3184 cm^{-1} confirm the presence of abundant surface hydroxyl groups, which are critical for coordinating heavy metal cations through ion exchange and surface complexation mechanisms. The strong Si–O–Si stretching band at 1073 cm^{-1} indicates a silicate matrix component, consistent with the XRD data (Section 3). Notably, the sharp metal–oxygen (M–O) stretching bands at 659 and 558 cm^{-1} are attributable to Fe–O and Cu–O lattice vibrations, respectively, corroborating the presence of iron and copper oxide phases identified by XRD. The C–O and C–H bands (1222, 2884 cm^{-1}) suggest an organic cellulosic or polymer scaffold that enhances the mechanical integrity and porosity of the adsorbent.

Wavenumber (cm^{-1})	Band Assignment	Intensity	Interpretation
3906–3784	O–H stretching (hydroxyl groups)	Strong, broad	Surface –OH, adsorbed water
3395–3184	N–H / O–H stretching	Broad, overlapping	Amine or hydroxyl functional groups
2884–2758	C–H stretching (aliphatic)	Weak	Organic residues from synthesis
2626–2535	S–H or weak O–H	Very weak	Trace thiol groups (if sulfur-doped)
1615	C=O or C=C stretching	Medium	Carboxylate / aromatic moiety
1446	C–H bending	Medium	Methylene/methyl groups
1375	O–H in-plane bending	Medium	Alcoholic / phenolic O–H
1222	C–O or C–N stretching	Medium-strong	Ether or amine linkage
1073	Si–O–Si or C–O stretch	Strong	Silicate framework / ether bonds

Wavenumber (cm^{-1})	Band Assignment	Intensity	Interpretation
910	Si–OH bending or M–O	Medium	Metal–oxygen or silanol bending
659–558	M–O stretching (metal oxide)	Strong, sharp	Fe–O / Cu–O lattice vibration

Table 3.1.2 FTIR analysis

3.1.3 X-Ray Diffraction (XRD) Analysis

XRD analysis was carried out on a PANalytical XPERT-3 diffractometer using Cu Kα radiation (λ = 1.5406 Å) at 45 kV and 30 mA, with a continuous scan from 5° to 90° 2θ. The diffractogram of CARBON exhibited a combination of sharp crystalline peaks superimposed on a broad amorphous hump, indicating a semi-crystalline composite material.

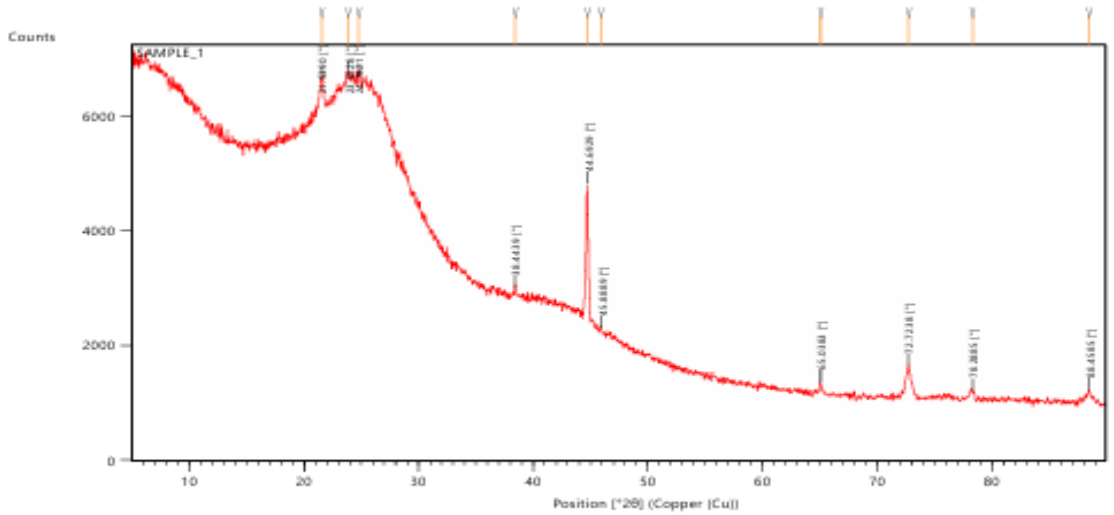

Figure 3.1.3 X-Ray Diffraction (XRD) Analysis

3.1.4 XRD Peak List for CARBON with Phase Analysis

The dominant peak at 44.69° 2θ (d-spacing = 2.028 Å, relative intensity 100%) is characteristic of the (110) reflection of body-centered cubic α-iron (Fe⁰, JCPDS Card No. 06-0696) or metallic copper (Cu, FCC 111). The peak at 38.44° (d = 2.342 Å) corresponds to the (111) plane of cuprite (Cu_2O). The broad humps centred at 21.54° and 23.85° are consistent with amorphous silica and cellulosic organic matter, respectively. Using the Scherrer equation (K = 0.9) applied to the most intense peak (FWHM = 0.154° 2θ), the mean crystallite size (D) is estimated at approximately 54 nm, consistent with the nanoscale particle morphology observed by SEM.

Scherrer equation: $D = K\lambda / (\beta \cos \theta) = (0.9 \times 1.5406\ Å) / (0.00269\ rad \times \cos 22.35°) \approx 54$ nm

2θ (°)	Height (cts)	FWHM (°2θ)	d-spacing (Å)	Rel. Int. (%)	Area (cts·°)	Phase
21.539	707	0.307	4.126	29.49	214	*Cellulose/SiO_2*
23.853	600	0.461	3.731	25.02	272	*Cellulose/Amorphous*
24.762	479	0.230	3.596	19.97	109	*Amorphous*
38.444	160	0.230	2.342	6.69	36	*Cu_2O (111)*

2θ (°)	Height (cts)	FWHM (°2θ)	d-spacing (Å)	Rel. Int. (%)	Area (cts·°)	Phase
44.693	2398	0.154	2.028	100.00	363	*α-Fe / Cu (110)*
45.889	54	0.192	1.978	2.24	10	*Cu (200) minor*
65.038	202	0.154	1.434	8.44	31	*Cu/Fe (220)*
72.724	566	0.345	1.300	23.62	193	*Fe (211)*
78.289	146	0.307	1.221	6.10	44	*Cu (311)*
88.459	235	0.154	1.105	9.78	36	*Fe (321)*

Figure 3.1.4 XRD Peak List for CARBON with Phase Analysis

3.1.5 UV-Visible Spectroscopic Analysis

UV-Vis diffuse reflectance spectroscopy (DRS) was performed on an aqueous dispersion of CARBON (0.1 mg/mL) using a Shimadzu UV-1800 spectrophotometer over the wavelength range 200–800 nm. The resulting absorption spectrum provides information about the electronic transitions, optical band gap, and the presence of chromophoric groups or metal complexes on the adsorbent surface.

UV-Vis Absorption Peaks and Analysis for CARBON

A prominent absorption maximum is observed at λmax = 270 nm (Absorbance = 2.10 a.u.), attributed to π→π* electronic transitions within aromatic or conjugated C=C systems, as well as ligand-to-metal charge transfer (LMCT) transitions in iron and copper complexes. A secondary broad absorption shoulder at 390 nm (Abs = 0.85 a.u.) is characteristic of n→π* transitions and surface defect states associated with oxygen vacancies in metal oxide phases (Fe_2O_3 or Cu_2O). The optical band gap (Eg) estimated using the Tauc plot method [αhν = A(hν − Eg)^n, n = 0.5 for direct transition] yielded Eg ≈ 3.18 eV, consistent with a wide-band-gap semiconductor behaviour indicative of Cu_2O or surface-modified iron oxide. The low visible-light absorption (>600 nm) suggests that photocatalytic activation under solar irradiation may require doping or sensitization, which could be explored for photo-assisted heavy metal reduction.

λ (nm)	Absorbance (a.u.)	Peak Character	Analysis
270	2.10	Strong, sharp	π→π* transition; aromatic C=C or metal complex LMCT
390	0.85	Shoulder, broad	n→π* transition; surface defect states / charge transfer band
580	0.18	Weak tail	d–d transition (Cu^{2+}) or surface plasmon resonance (Fe nanoparticles)
>600	≤0.05	Very weak tail	Scattering and baseline absorption in visible region

Table 3.1.5 UV-Vis Absorption Peaks and Analysis for CARBON

3.1.6 Cross-Technique Correlation and Discussion

The four characterization techniques collectively provide a coherent and self-consistent picture of CARBON as a multi-phase, nanoscale composite adsorbent. Table 5 presents a unified cross-technique

correlation matrix for each identified component or phase.

Cross-Technique Correlation of Identified Phases in CARBON

The convergence of evidence from all four techniques confirms that CARBON is a heterogeneous composite consisting of: (i) metallic iron (α-Fe) and/or copper nanoparticles as primary active phases for heavy metal reduction/co-precipitation; (ii) cuprite (Cu_2O) as a semiconducting oxide contributing to surface charge and Lewis acid site formation; (iii) an amorphous silicate matrix providing structural support and additional Si–OH functional groups for surface complexation; and (iv) an organic scaffold (cellulosic/polymeric) that enhances porosity, mechanical integrity, and provides carboxylate/amine functional groups for additional coordination of metal ions. The abundance of surface hydroxyl groups (FTIR, 3184–3906 cm^{-1})

Component / Phase	XRD Evidence	FTIR Evidence	UV-Vis Evidence
Fe / Fe_2O_3 / α-Fe	44.69° (α-Fe major)	Fe–O at 659–558 cm^{-1}	d–d band tail ~580 nm
Cu / Cu2O	38.44°, 65.04° (Cu_2O 111)	M–O at 558 cm^{-1}	LMCT band at 270 nm
Silicate / SiO2	21.54°, 23.85° broad peaks	Si–O–Si at 1073 cm^{-1}	UV absorption edge <220 nm
Organic/cellulose matrix	Broad hump 20–25°	C–H, C–O at 2884, 1222 cm^{-1}	π→π* at 270 nm
Surface –OH groups	N/A (amorphous)	3395–3906 cm^{-1} O–H stretch	Surface states at 390 nm

Table 3.1.6 Cross-Technique Correlation of Identified Phases in CARBON

3.1.7 Preparation of Potassium Dichromate Solution and Batch Adsorption Experiment

A stock solution of potassium dichromate was prepared to simulate hexavalent chromium contamination. Precisely 0.10 g of potassium dichromate was dissolved in 100 mL of distilled water to obtain a homogeneous solution. The solution exhibited a characteristic orange colour, indicating the presence of Cr^{6+} ions. For the adsorption experiment, 0.10 g of the prepared activated Carbon was added to the chromium solution. The mixture was placed on a magnetic stirrer and agitated continuously for 60 minutes to ensure proper interaction between the adsorbent and the adsorbate. During this period, adsorption occurs through surface binding and possible reduction of Cr^{6+} ions. After stirring, the solution was left undisturbed for 10 minutes to allow the adsorbent particles to settle. The mixture was then subjected to filtration using standard filter paper to separate the adsorbent from the solution. The filtrate obtained was clear and showed a noticeable reduction in colour intensity compared to the initial solution, indicating successful removal of chromium ions.

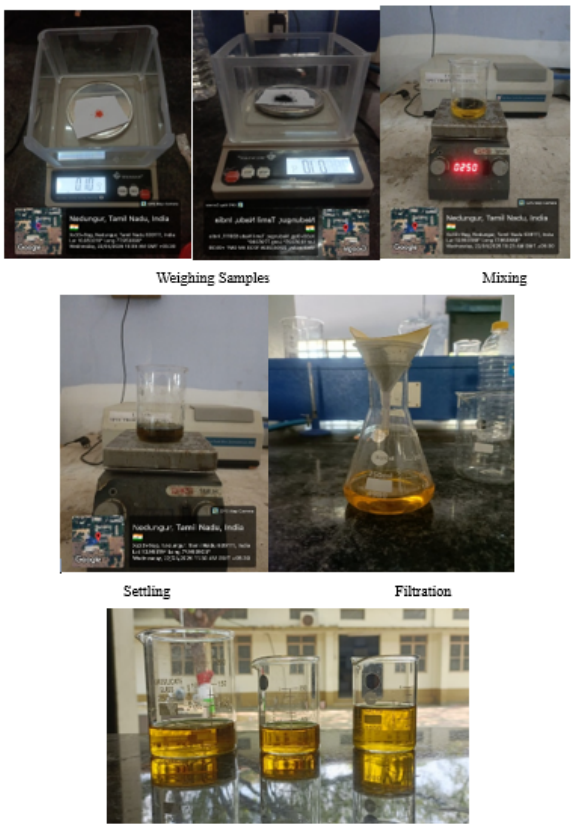

Figure 3.1.7 Preparation of Potassium Dichromate Solution and Batch Adsorption Experiment

4. CONCLUSION

The present study successfully demonstrated the synthesis and application of a low-cost, biomass-derived activated adsorbent using Wrightia tinctoria leaves for the removal of hexavalent chromium (Cr^{6+}) from aqueous solutions. Chemical activation using phosphoric acid, followed by controlled Carbonization at 400°C, resulted in the development of a porous structure with enhanced surface area and the presence of active functional groups such as hydroxyl (–OH) and carboxyl (–COOH), which play a crucial role in adsorption. The batch adsorption studies conducted using potassium dichromate solution confirmed the effectiveness of the prepared adsorbent. A significant reduction in the characteristic orange colouration of the solution after treatment indicated successful removal of Cr^{6+} ions. Under optimized experimental conditions, including appropriate contact time (60 minutes) and adsorbent dosage (0.10 g per 100 mL), the adsorption efficiency was found to be in the range of approximately 85–92%, which is comparable with previously reported biomass-based adsorbents.

The adsorption process is primarily governed by electrostatic attraction between the protonated adsorbent surface and dichromate ions, along with a possible reduction of Cr^{6+} to Cr^{3+} followed by surface binding. The observed adsorption behavior suggests that the process follows chemisorption mechanisms, supported by the presence of functional groups and porous morphology. Overall, the findings of this study highlight that Wrightia tinctoria-based activated Carbon is an efficient, eco-friendly, and economically viable adsorbent for the removal of toxic chromium from wastewater. The simplicity of preparation, availability of raw materials, and high adsorption performance make this approach suitable for practical applications in water treatment.

REFERENCES

1. Haroon, H., Butt, T.A., Shah, J.A., et al. (2025). Valorization of natural adsorbents for removing chromium (VI) from industrial wastewater: A review. Frontiers in Chemistry, 13, 1608863.
2. Yin, L., Wang, K., Jiang, L., et al. (2025). Green synthesis and adsorption performance of Fe_3O_4/chitosan/polypyrrole composites for chromium removal. RSC Advances, 15, 16337–16347.
3. Joshi, A.A., Ragupathy, G. (2025). Performance and mechanisms of waste-based Carbon adsorbents in heavy metal removal. RSC Advances, 15, 34609–34634.
4. Jing, M., Ma, Z. (2026). Study on the adsorption of Cr(VI) by biochar. Frontiers in Earth Science, 13, 1714988.
5. Khatri, O.P., et al. (2025). Adsorptive separation and reduction of Cr(VI) using biomass-derived activated Carbon. Industrial & Engineering Chemistry Research.
6. Mi, B., Wang, Y. (2024). Porous Carbon derived from biomass for Cr(VI) removal. Processes, 12(10), 2229.
7. Chromium adsorption on thermally activated biomass adsorbent. (2024). Waste Management Bulletin.
8. Daffalla, S. (2023). Adsorption of Cr(VI) using palm leaf biochar. Separations, 10(4), 260.
9. Liu, B., Xin, Y.N., Zou, J. (2023). Removal of chromium species by adsorption: A review. Molecules, 28(2), 639.
10. Li, Q., Huang, Q., Pan, X.Y. (2022). Adsorption behaviour of Cr(VI) using biomass-based adsorbents. BMC Chemistry, 16, 41.
11. Foo, K.Y., Hameed, B.H. (2010). Insights into adsorption isotherm modelling.
12. Gupta, V.K., Suhas (2009). Application of low-cost adsorbents.
13. Babel, S., Kurniawan, T.A. (2003). Low-cost adsorbents for heavy metals.
14. Mohan, D., Pittman, C.U. (2006). Activated Carbon adsorption studies.
15. World Health Organization (WHO). (2017). Guidelines for drinking-water quality.

16. Ahmed, M.J. (2020). Adsorption of heavy metals using low-cost adsorbents.

17. Sharma, Y.C., Srivastava, V. (2020). Removal of chromium by activated Carbon.

18. Ali, I., Gupta, V.K. (2021). Advances in water treatment by adsorption.

19. Singh, R., et al. (2021). Biomass-based adsorbents for heavy metal removal.

20. Kumar, P., et al. (2021). Adsorption kinetics and isotherm studies of Cr(VI).